Scalar Reduction of a Neural Field Model with Spike Frequency Adaptation

Youngmin Park & Bard Ermentrout

University of Pittsburgh Department of Mathematics

yop6@pitt.edu

October 29, 2017

Introduction: T-Maze Task Decision

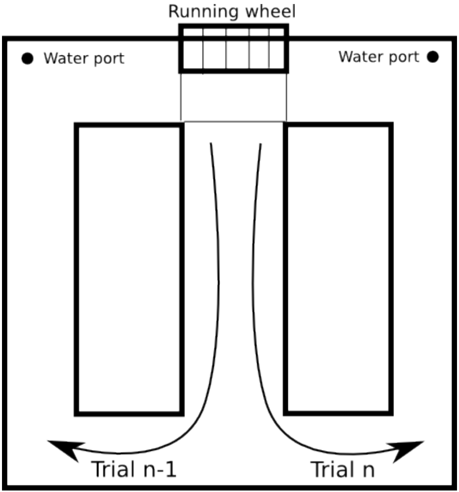

Introduction: T-Maze Task Reward

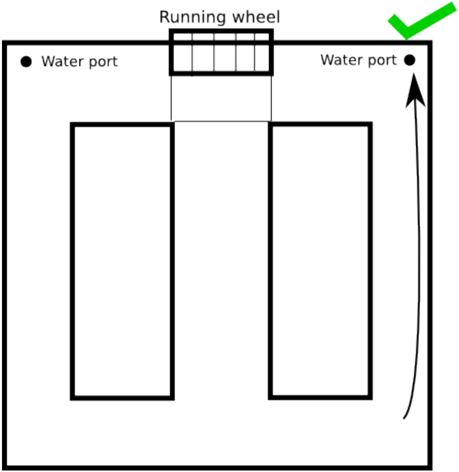

Introduction: T-Maze Task Return to Wheel

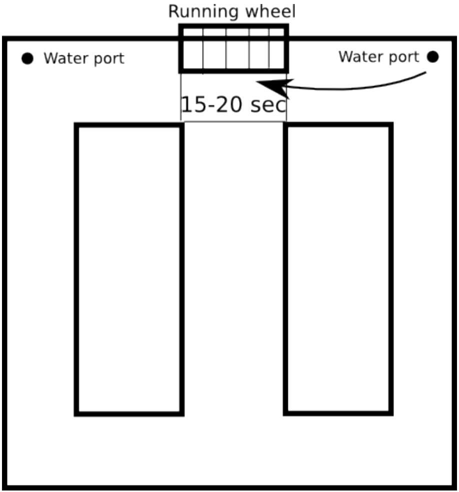

Introduction: Data During Wheel Running

- Hippocampal neurons can produce reliable, long-lasting transient (∼10 sec) firing patterns without external stimuli.

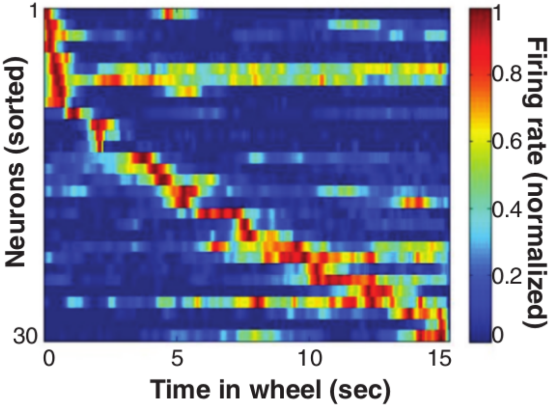

Figure: Pastalkova et al. (2008).

Introduction: A Mechanism for Sequential Neural Spiking

- Itskov et al. (2011) investigated the mechanism behind this sequence generation.
- Threshold adaptation model:

$$\dot{x}_i = -x_i + \left[\sum_{j=1}^{N} J_{ij}x_j + I_i - h_i\right]_+$$
$$\dot{h}_i = \frac{1}{2000}(-h_i + 0.5x_i),$$

- J is the network of synaptic weights, I is a time-dependent vector of external inputs, and h_i is an adaptation variable.

Introduction: Synaptic Weights

$$\dot{x}_i = -x_i + \left[\sum_{j=1}^{N} J_{ij} x_j + I_i - h_i\right]_+$$

$$\dot{h}_i = \frac{1}{2000}(-h_i + 0.5x_i),$$

- The synaptic weights depend on the distance from a given neuron ("Mexican Hat" function)

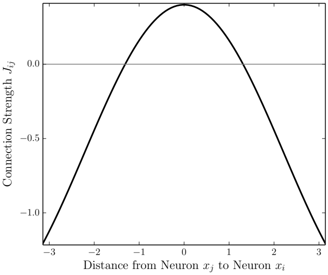

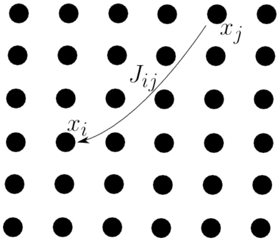

Introduction: Model Solutions

Introduction: Model Solutions

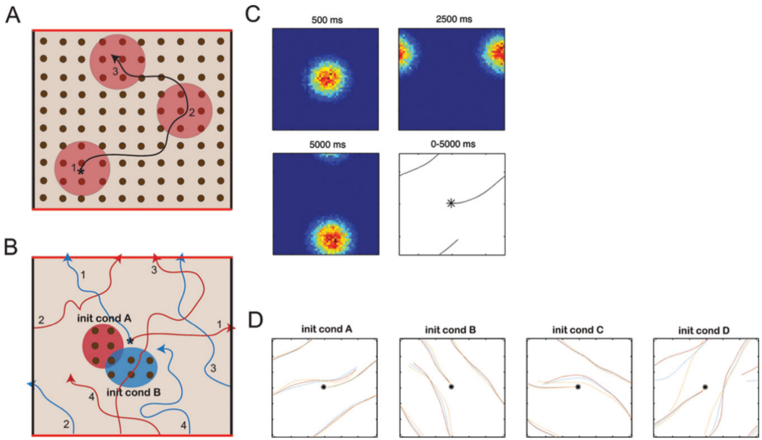

Figure: Itskov et al. (2011)

Introduction: Mathematical Goals

Using an idealized model...

- Prove elementary properties like existence, uniqueness, and stability of steady-state bump solutions.
- Prove existence and stability of other behaviors like traveling bumps.

Introduction: Neural Field Model

In our study, we considered this neural field model first studied by Pinto and Ermentrout (2001)

$$
\begin{aligned}
\frac{\partial u(\mathbf{x},t)}{\partial t} &= -u(\mathbf{x},t) + \int_\Omega K(\mathbf{x}-\mathbf{y}) f(u(\mathbf{y},t))\, d\mathbf{y} \\
&+ \varepsilon[qI(\mathbf{x}) - gz(\mathbf{x},t)], \\
\frac{\partial z(\mathbf{x},t)}{\partial t} &= \varepsilon[-z(\mathbf{x},t) + u(\mathbf{x},t)],
\end{aligned}
$$

- Periodic boundary conditions on Ω (unit circle or torus).

Introduction: Neural Field Model

In our study, we considered this neural field model first studied by Pinto and Ermentrout (2001)

$$\begin{aligned}\frac{\partial u(\mathbf{x},t)}{\partial t} &= -u(\mathbf{x},t) + \int_\Omega K(\mathbf{x}-\mathbf{y}) f(u(\mathbf{y},t))\, d\mathbf{y} \\ &+ \varepsilon[qI(\mathbf{x}) - gz(\mathbf{x},t)], \\ \frac{\partial z(\mathbf{x},t)}{\partial t} &= \varepsilon[-z(\mathbf{x},t) + u(\mathbf{x},t)],\end{aligned}$$

- Periodic boundary conditions on Ω (unit circle or torus).
- K even, periodized Mexican hat on Ω, f sigmoidal.

Introduction: Neural Field Model

In our study, we considered this neural field model first studied by Pinto and Ermentrout (2001)

$$
\begin{aligned}
\frac{\partial u(\mathbf{x},t)}{\partial t} &= -u(\mathbf{x},t) + \int_\Omega K(\mathbf{x}-\mathbf{y}) f(u(\mathbf{y},t))\, d\mathbf{y} \\
&+ \varepsilon[qI(\mathbf{x}) - gz(\mathbf{x},t)], \\
\frac{\partial z(\mathbf{x},t)}{\partial t} &= \varepsilon[-z(\mathbf{x},t) + u(\mathbf{x},t)],
\end{aligned}
$$

- Periodic boundary conditions on Ω (unit circle or torus).
- K even, periodized Mexican hat on Ω, f sigmoidal.
- $0 < \varepsilon \ll 1$,

Introduction: Neural Field Model

In our study, we considered this neural field model first studied by Pinto and Ermentrout (2001)

$$\begin{aligned}
\frac{\partial u(\mathbf{x},t)}{\partial t} &= -u(\mathbf{x},t) + \int_\Omega K(\mathbf{x}-\mathbf{y}) f(u(\mathbf{y},t))\, d\mathbf{y} \\
&+ \varepsilon[qI(\mathbf{x}) - gz(\mathbf{x},t)], \\
\frac{\partial z(\mathbf{x},t)}{\partial t} &= \varepsilon[-z(\mathbf{x},t) + u(\mathbf{x},t)],
\end{aligned}$$

- Periodic boundary conditions on Ω (unit circle or torus).
- K even, periodized Mexican hat on Ω, f sigmoidal.
- $0 < \varepsilon \ll 1$,
- g, q represent the strength of adaptation and input current, respectively.

One-dimensional Example Solutions

One-dimensional Example Solutions

Two-dimensional Example Solutions

Results on Existence and Stability are Known

- Existence, uniqueness, and stability of steady-state bump solutions. Zhang and Wu (2012); Pinto and Ermentrout (2001)
- Existence and stability of traveling bump solutions Kilpatrick and Bressloff (2010); Fung and Amari (2015)
- The existence of many other spatio-temporal dynamics including traveling waves, spiral waves, breathers, and pulse emitters have been shown to exist Bressloff et al. (2003); Folias and Bressloff (2004, 2005a,b,a); Folias (2017); Kilpatrick and Bressloff (2010, 2009); Bressloff and Folias (2004); Bressloff et al. (2003); Kilpatrick and Bressloff (2009).

Restrictive Assumptions on Existing Results

$$\begin{aligned}
\frac{\partial u(\mathbf{x},t)}{\partial t} &= -u(\mathbf{x},t) + \int_\Omega K(\mathbf{x}-\mathbf{y}) f(u(\mathbf{y},t))\, d\mathbf{y} \\
&+ \varepsilon[qI(\mathbf{x}) - gz(\mathbf{x},t)], \\
\frac{\partial z(\mathbf{x},t)}{\partial t} &= \varepsilon[-z(\mathbf{x},t) + u(\mathbf{x},t)],
\end{aligned}$$

- However, these studies assume a discontinuous, switch-like firing rate f, thus classical dynamical systems theory does not always apply.
- These studies often place particular assumptions on the choice of kernel K.

- We seek to reduce the dimensionality of the model to the coordinates of the centroid.

$$u(\mathbf{x}, t) = U_0(x_1 + \theta_1, x_2 + \theta_2) + \varepsilon U_1(\mathbf{x}, t) + O(\varepsilon^2).$$

- U_0 is the steady-state bump solution, the term $\varepsilon U_1(\mathbf{x}, t)$ represents small amplitude deviations from U_0, and the terms θ_1 and θ_2 represent drifts of the centroid.
- Using the method of multiple timescales (Keener (1988)), we derive the dynamics of θ_1, θ_2.
- Note: This expansion and the method of multiple timescsales does not require strong assumptions on f or K.

Phase Equations

The time-drift in the centroid of the bump solution is given by the differential equations,

$$\theta_i' = qJ_i(\boldsymbol{\theta}) - g\int_0^\tau e^{-(\tau-s)}H_i(\boldsymbol{\theta}(s)-\boldsymbol{\theta}(\tau))ds, \quad i=1,2,$$

where

$$\begin{aligned} J_i(\boldsymbol{\theta}) &= \int_\Omega f'(u_0(\mathbf{x}+\boldsymbol{\theta}))\partial_i u_0(\mathbf{x}+\boldsymbol{\theta})I(\mathbf{x})\ d\mathbf{x}, \\ H_i(\boldsymbol{\theta}) &= \int_\Omega f'(u_0(\mathbf{x}))\partial_i u_0(\mathbf{x})u_0(\mathbf{x}+\boldsymbol{\theta})\ d\mathbf{x}, \end{aligned}$$

and $\boldsymbol{\theta} = (\theta_1, \theta_2)$, $\tau = \varepsilon t$.
We aim to use the reduction to classify the existence and stability of bump solutions.

Neural Field on the 1D Domain: Parameter Space

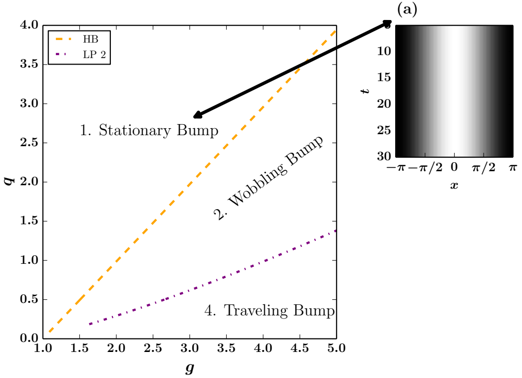

Neural Field on the 1D Domain: Parameter Space

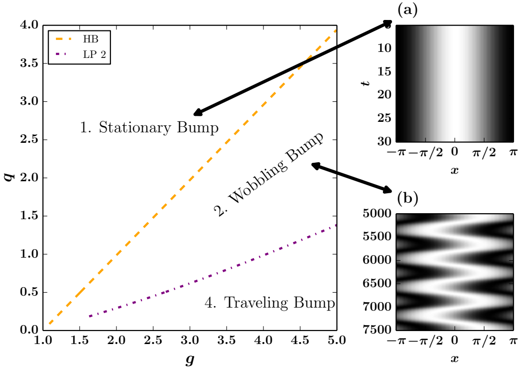

Neural Field on the 1D Domain: Parameter Space

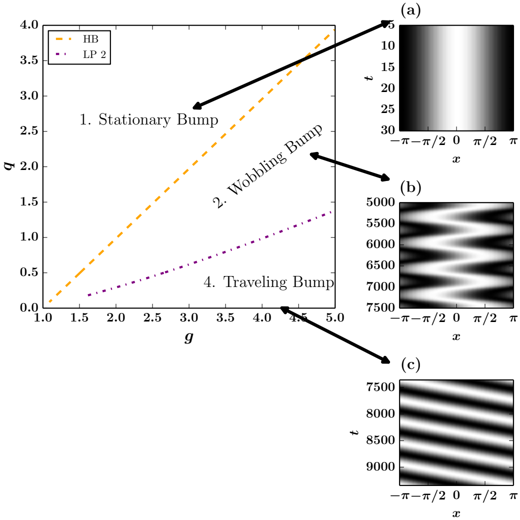

Neural Field on the 1D Domain: Parameter Space

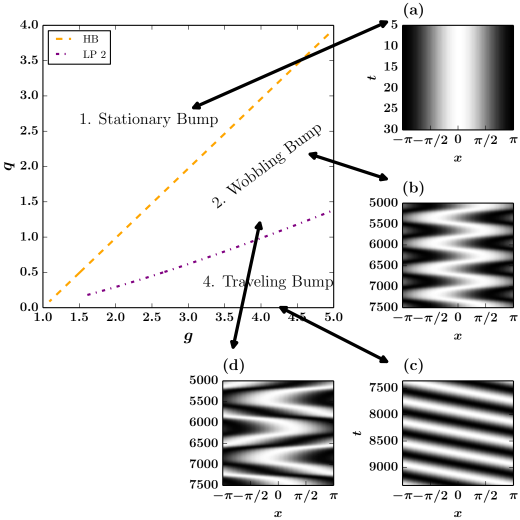

Neural Field on the 1D Domain: Parameter Space

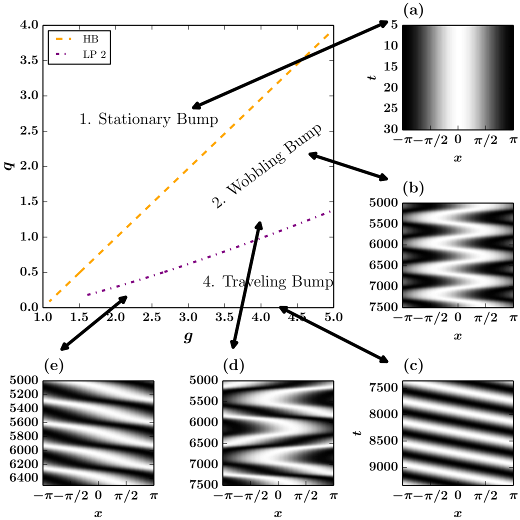

Reduced Neural Field on the 1D Domain: Parameter Space

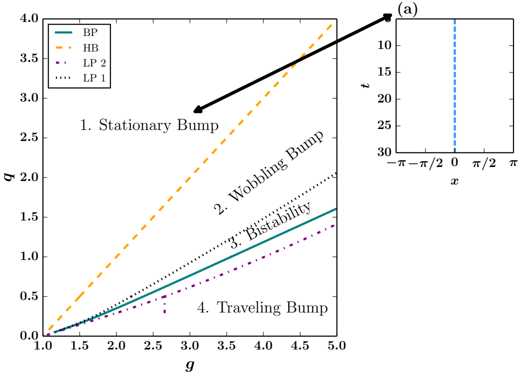

Reduced Neural Field on the 1D Domain: Parameter Space

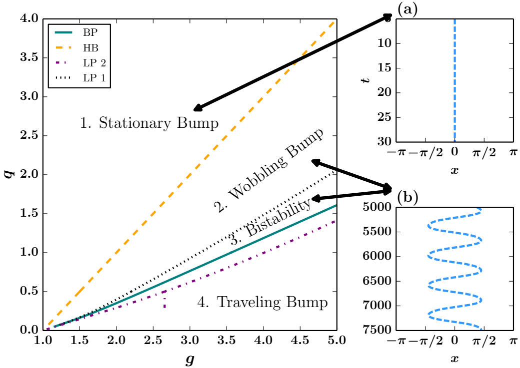

Reduced Neural Field on the 1D Domain: Parameter Space

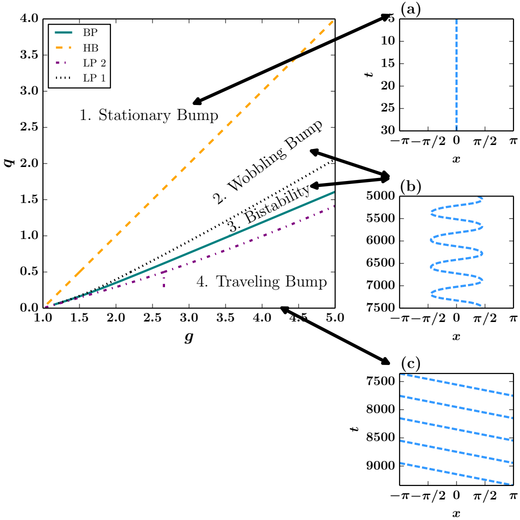

Reduced Neural Field on the 1D Domain: Parameter Space

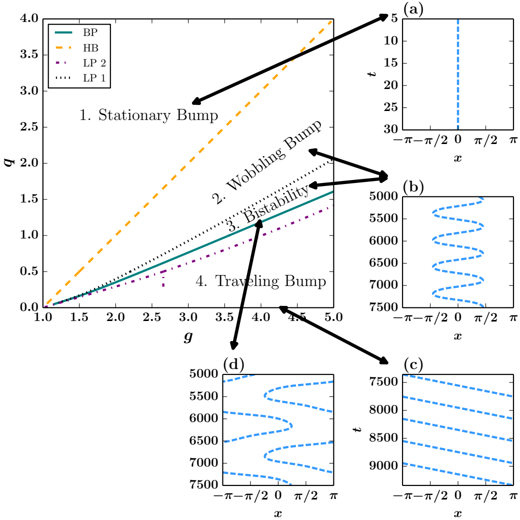

Reduced Neural Field on the 1D Domain: Parameter Space

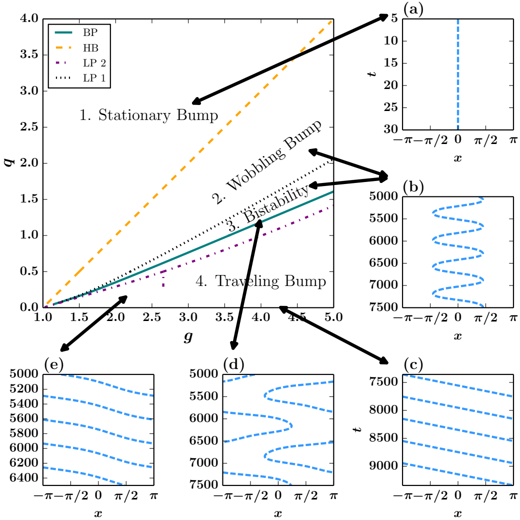

Reduced Neural Field vs Full Neural Field

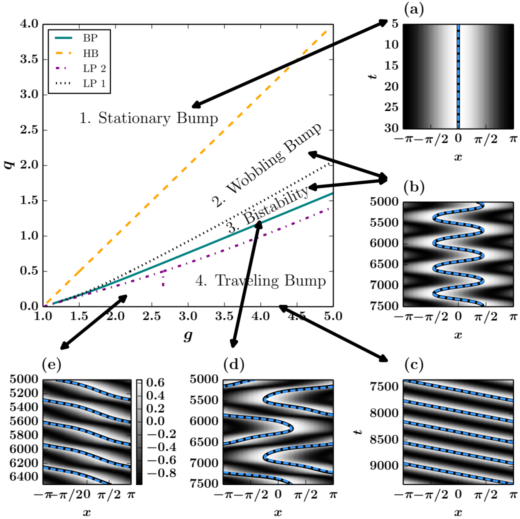

Analytical Results on the 1D Domain: Oscillations

First, existence of a Hopf bifurcation: Let $\theta = 0 + \varepsilon e^{\lambda\tau}$. Plug this expansion into the phase to get an equation for λ.

$$\lambda^2 + \lambda[1 - qJ'(0) - gH'(0)] - qJ'(0) = 0$$

Generally, $J'(0) < 0$ and $H'(0) > 0$, so there exists a Hopf bifurcation when

$$g^* = \frac{1 - qJ'(0)}{H'(0)}.$$

with q sufficiently large.

Existence and stability of oscillations follows from a normal form analysis.

Analytical Results on the 1D Domain: Traveling Solutions

Suppose $q = 0$ and $g > 0$ and let $\theta(\tau) = \nu\tau$. If we choose $K(x) = A + B\cos(x)$, then $H(x) = \sin(x)$. Plugging in yields an equation for the velocity of the bump solution as a function of adaptation g.

$$\begin{aligned}\nu &= -g\int_0^\infty e^{-s}H(-\nu s)ds \\ &= g\int_0^\infty e^{-s}\sin(-\nu s)ds \\ &= \frac{g\nu}{1+\nu^2}.\end{aligned}$$

So $\nu = \pm\sqrt{g-1}$

Conclusion of Analysis on the 1D domain

- The phase model faithfully reproduces the dynamics of the neural field model
- The phase model allows for a much more straightforward analysis for the existence of particular dynamics
  - Existence of sloshing solutions via a Hopf bifurcation.
  - Stability of sloshing solutions via a normal form analysis.
  - Existence of constant velocity traveling solutions.
  - Existence and stability of non-constant velocity traveling solutions.

Qualitative Dynamics on the Two-dimensional Domain

- A direct numerical analysis of the neural field model on a two-dimensional domain is not tractable.

Qualitative Dynamics on the Two-dimensional Domain

- A direct numerical analysis of the neural field model on a two-dimensional domain is not tractable.
- To make the numerics tractable, we take a Fourier truncation of the kernel K,

$$K(\mathbf{x}) = k_{00} + k_{10}\cos(x_1) + k_{01}\cos(x_2) + k_{11}\cos(x_1)\cos(x_2),$$

which allows us to rewrite the neural field equations on the 2D domain into a system of 18 ODEs.

Qualitative Dynamics on the Two-dimensional Domain

- A direct numerical analysis of the neural field model on a two-dimensional domain is not tractable.
- To make the numerics tractable, we take a Fourier truncation of the kernel K,

$$K(\mathbf{x}) = k_{00} + k_{10}\cos(x_1) + k_{01}\cos(x_2) + k_{11}\cos(x_1)\cos(x_2),$$

  which allows us to rewrite the neural field equations on the 2D domain into a system of 18 ODEs.
- Although the numerics are more tractable and compatible with existing numerical packages like AUTO, we are unable to generate a two parameter bifurcation diagram.

Neural Field on the 2D Domain: Parameter Space

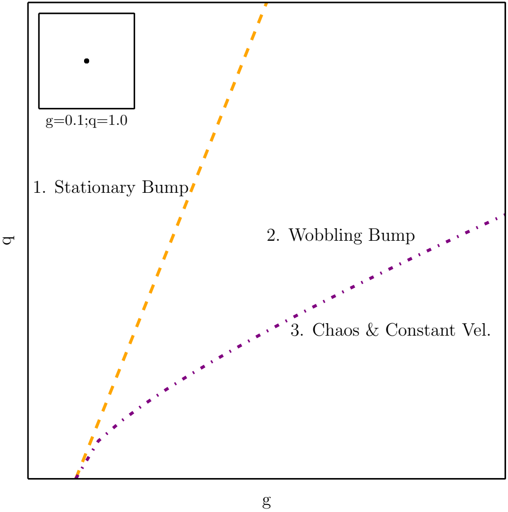

Neural Field on the 2D Domain: Parameter Space

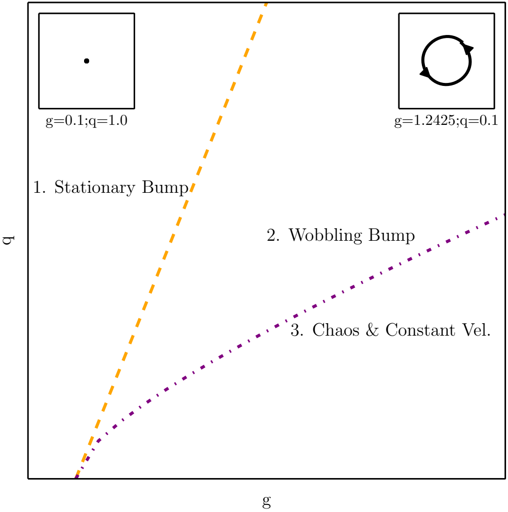

Neural Field on the 2D Domain: Parameter Space

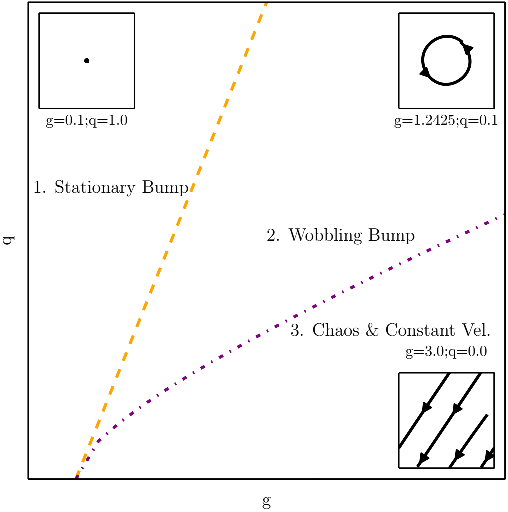

Neural Field on the 2D Domain: Parameter Space

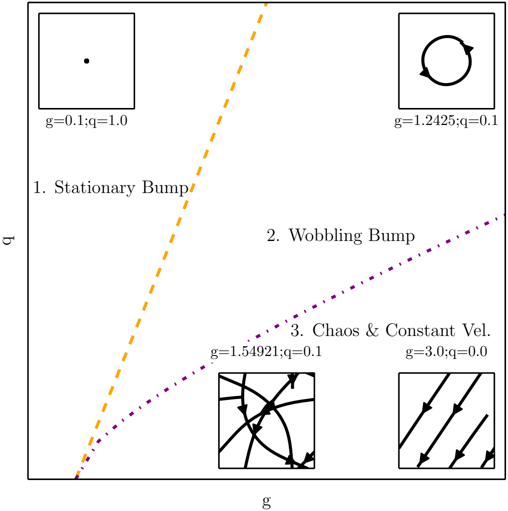

2D Domain: Approximation of the Phase Equations

$$\frac{d\theta_i}{d\tau} = qJ_i(\boldsymbol{\theta}) - g\int_0^\tau e^{-(\tau-s)} H_i(\boldsymbol{\theta}(s) - \boldsymbol{\theta}(\tau))ds, \quad i = 1, 2,$$

- The Fourier truncation of the kernel results in the Fourier truncation of H_i,

$$H_1(\theta_1, \theta_2) = \sin(\theta_1)(h_{10} + h_{11}\cos(\theta_2))$$
$$H_2(\theta_1, \theta_2) = \sin(\theta_2)(h_{10} + h_{11}\cos(\theta_1)).$$

2D Domain: Approximation of the Phase Equations

$$\frac{d\theta_i}{d\tau} = qJ_i(\boldsymbol{\theta}) - g\int_0^\tau e^{-(\tau-s)}H_i(\boldsymbol{\theta}(s)-\boldsymbol{\theta}(\tau))ds, \quad i=1,2,$$

- The Fourier truncation of the kernel results in the Fourier truncation of H_i,

$$H_1(\theta_1,\theta_2) = \sin(\theta_1)(h_{10} + h_{11}\cos(\theta_2))$$
$$H_2(\theta_1,\theta_2) = \sin(\theta_2)(h_{10} + h_{11}\cos(\theta_1)).$$

- We can then rewrite the phase equations as a system of 10 ODEs and generate bifurcation diagrams using AUTO.

Neural Field on the 2D Domain: Parameter Space

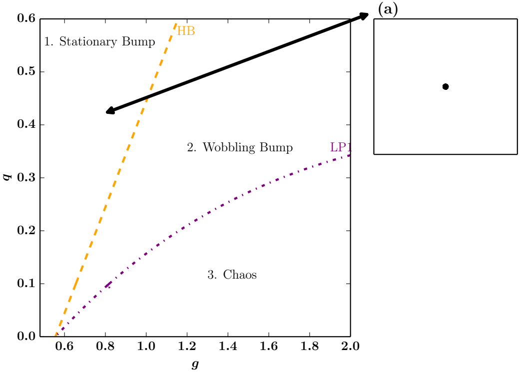

Reduced Neural Field on the 2D Domain: Parameter Space

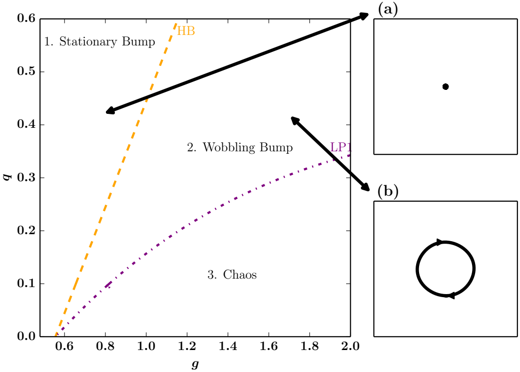

Reduced Neural Field on the 2D Domain: Parameter Space

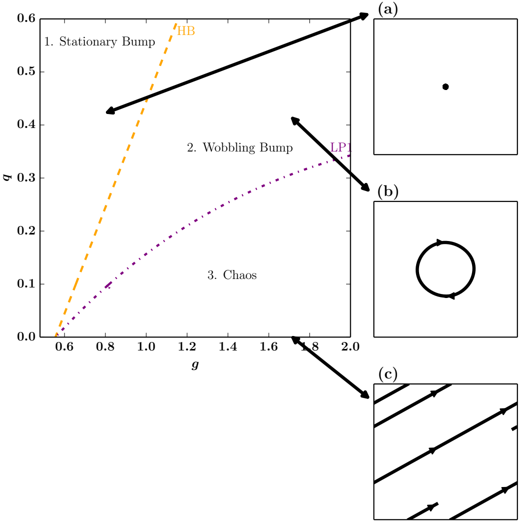

Reduced Neural Field on the 2D Domain: Parameter Space

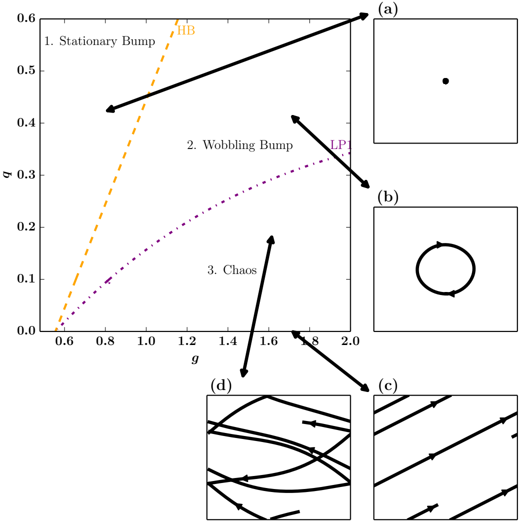

Reduced Neural Field on the 2D Domain: Parameter Space

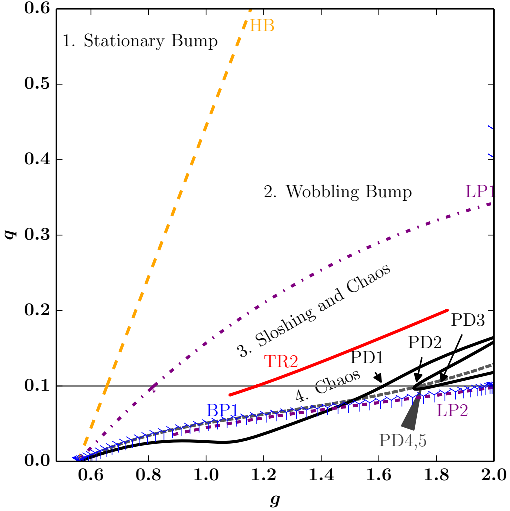

Analytical Results on the 2D Domain

Let $q = 0$ and consider the ansatz $\theta_1(\tau) = \nu_1 \tau$ and $\theta_2(\tau) = \nu_2 \tau$. Constant velocity bump solutions exist if ν_1, ν_2 simultaneously satisfy

$$\nu_1 = g \int_0^\infty e^{-s} H_1(\nu_1 s, \nu_2 s) ds,$$
$$\nu_2 = g \int_0^\infty e^{-s} H_2(\nu_1 s, \nu_2 s) ds.$$

If we take $H_1(\theta_1, \theta_2) = \sin(\theta_1)(h_{10} + h_{11} \cos(\theta_2))$ and $H_2(\theta_1, \theta_2) = \sin(\theta_2)(h_{10} + h_{11} \cos(\theta_1))$, we can solve for ν_1, ν_2 explicity.

Analytical Results on the 2D Domain: Constant Velocity Solutions (Existence)

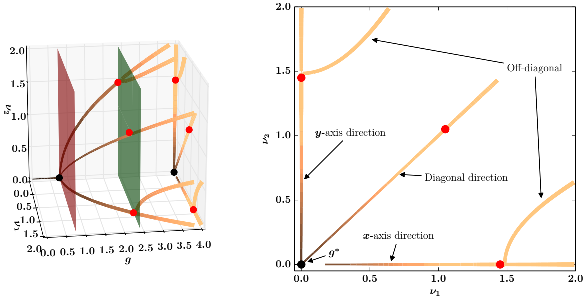

Figure: Existence of traveling bump solutions using the truncated interaction function H_i^F. After a critical value g^*, there exist traveling bumps in the axial directions and the diagonal directions. After a second critical value of g (marked by a vertical gray line), off-diagonal solutions form and continue to persist for large g.

Conclusion of Analysis on the 2D domain

- The phase model qualitatively reproduces the dynamics of the neural field model.
- As in the 1D domain, the phase model allows for a much more straightforward analysis for the existence of particular dynamics
  - Existence of sloshing solutions via a Hopf bifurcation.
  - Existence of constant velocity traveling solutions.
  - Existence and stability of non-constant velocity traveling solutions.

Conclusion

- We successfully reduce the dimensionality of the model to one or two scalar differential equations representing the coordinates of the centroid.
- This reduction places no strong assumptions on the firing rate function or the kernel.
- Using this reduction, we show that it faithfully reproduces the dynamics of the original neural field model, and we use it to rigorously classify the existence and stability of various bump dynamics.

,

Acknowledgements

- NSF DMS 1712922
- Maria N. Geffen
- G. Bard Ermentrout

Thanks to members of the Pitt math bio group

- Jon Rubin
- Brent Doiron
- Abby Pekoske
- Marcello Codiani
- Jay Pina

and visiting scholars

- Cati Vich (Universitat De Les Illes Balears)
- Aki Akao (Univ. of Tokyo)

Paul C. Bressloff and Stefanos E Folias. Front bifurcations in an excitatory neural network. *SIAM Journal on Applied Mathematics*, 65(1):131–151, January 2004. ISSN 0036-1399. doi: 10.1137/S0036139903434481. URL http://epubs.siam.org/doi/abs/10.1137/S0036139903434481.

Paul C. Bressloff, Stefanos E Folias, A. Prat, and Y.-X. Li. Oscillatory waves in inhomogeneous neural media. *Physical Review Letters*, 91(17): 178101, October 2003. doi: 10.1103/PhysRevLett.91.178101. URL http://link.aps.org/doi/10.1103/PhysRevLett.91.178101.

Stefanos E Folias. Traveling waves and breathers in an excitatory-inhibitory neural field. *Physical Review E*, 95(3):032210, 2017.

Stefanos E Folias and Paul C. Bressloff. Breathing pulses in an excitatory neural network. *SIAM Journal on Applied Dynamical Systems*, 3(3): 378–407, January 2004. doi: 10.1137/030602629. URL http://epubs.siam.org/doi/abs/10.1137/030602629.

Stefanos E Folias and Paul C. Bressloff. Breathers in two-dimensional neural media. *Physical Review Letters*, 95(20):208107, November 2005a. doi: 10.1103/PhysRevLett.95.208107. URL http://link.aps.org/doi/10.1103/PhysRevLett.95.208107.

Stefanos E Folias and Paul C. Bressloff. Stimulus-locked traveling waves and breathers in an excitatory neural network. *SIAM Journal on Applied Mathematics*, 65(6):2067–2092, January 2005b. ISSN 0036-1399. doi: 10.1137/040615171. URL http://epubs.siam.org/doi/abs/10.1137/040615171.

C. C. A. Fung and S. i Amari. Spontaneous Motion on Two-Dimensional Continuous Attractors. *Neural Computation*, 27(3):507–547, March 2015. ISSN 0899-7667. doi: 10.1162/NECO_a_00711.

Vladimir Itskov, Carina Curto, Eva Pastalkova, and György Buzsáki. Cell assembly sequences arising from spike threshold adaptation keep track of time in the hippocampus. *The Journal of Neuroscience*, 31(8): 2828–2834, 2011.

James P Keener. *Principles of applied mathematics*. Addison-Wesley, 1988.

Zachary P. Kilpatrick and Paul C. Bressloff. Spatially structured oscillations in a two-dimensional excitatory neuronal network with synaptic depression. *Journal of Computational Neuroscience*, 28(2): 193–209, October 2009. ISSN 0929-5313, 1573-6873. doi: 10.1007/s10827-009-0199-6. URL `http://link.springer.com/article/10.1007/s10827-009-0199-6`.

Zachary P. Kilpatrick and Paul C. Bressloff. Effects of synaptic depression and adaptation on spatiotemporal dynamics of an excitatory neuronal network. *Physica D: Nonlinear Phenomena*, 239(9):547–560, May 2010. ISSN 0167-2789. doi: 10.1016/j.physd.2009.06.003. URL `http://www.sciencedirect.com/science/article/pii/S0167278909001833`.

Eva Pastalkova, Vladimir Itskov, Asohan Amarasingham, and György Buzsáki. Internally generated cell assembly sequences in the rat hippocampus. *Science*, 321(5894):1322–1327, 2008.

D. Pinto and G. Bard Ermentrout. Spatially structured activity in synaptically coupled neuronal networks: I. Traveling fronts and pulses. *SIAM Journal on Applied Mathematics*, 62(1):206–225, January 2001. ISSN 0036-1399. doi: 10.1137/S0036139900346453. URL `http://epubs.siam.org/doi/abs/10.1137/S0036139900346453`.

Wenhao Zhang and Si Wu. Neural information processing with feedback modulations. *Neural Computation*, 24(7):1695–1721, March 2012. ISSN 0899-7667. doi: 10.1162/NECO_a_00296. URL `http://www.mitpressjournals.org/doi/full/10.1162/NECO_a_00296`.

Derivation of the Phase Equations

To reduce the neural field, we consider slow timescale shifts in the bump solution,

$$\begin{aligned} U(\mathbf{x},\tau,\varepsilon) &= U_0(\mathbf{x},\tau) + \varepsilon U_1(\mathbf{x},\tau) + O(\varepsilon^2) \\ &= u_0(\mathbf{x} + \boldsymbol{\theta}(\tau)) + \varepsilon U_1(\mathbf{x},\tau) + O(\varepsilon^2) \end{aligned}$$

where $\tau = \varepsilon t$, and u_0 is the translation-invariant steady-state solution.

Derivation of the Phase Equations

Substituting this power series into the neural field model, we get:

$$\begin{aligned} 0 &= -U_0(\mathbf{x},\tau) + \int_\Omega K(\mathbf{x}-\mathbf{y}) f(U_0(\mathbf{y},\tau)) d\mathbf{y} \\ (L_0 U_1)(\mathbf{x},\tau) &= \frac{\partial U_0(\mathbf{x},\tau)}{\partial \tau} - qI(\mathbf{x}) + g \int_0^\tau e^{-(\tau-s)} U_0(\mathbf{x},s)\ ds, \end{aligned}$$

where

$$(L_0 v)(\mathbf{x}) = -v(\mathbf{x}) + \int_\Omega K(\mathbf{x}-\mathbf{y}) f'(U_0(\mathbf{y})) v(\mathbf{y})\ d\mathbf{y}.$$

Derivation of the Phase Equations

The linear operator L_0 has a nontrivial nullspace spanned by $\partial_i u_0(\mathbf{x})$, $i = 1, 2$, so we can not immediately say that there exists a solution to the equation

$$(L_0 U_1)(\mathbf{x}, \tau) = \frac{\partial U_0(\mathbf{x}, \tau)}{\partial \tau} - qI(\mathbf{x}) + g \int_0^\tau e^{-(\tau - s)} U_0(\mathbf{x}, s)\, ds.$$

Derivation of the Phase Equations

Recall the Fredholm Alternative which states that the equation

$$(L_0 v)(\mathbf{x}) = b(\mathbf{x})$$

has a bounded solution if and only if

$$\langle v_i^*(\mathbf{x}), b(\mathbf{x}) \rangle = 0$$

for $i = 1, 2$, where v^* is in the nullspace of the adjoint L^*, and $\langle \cdot, \cdot \rangle$ is the natural inner product,

$$\langle u(\mathbf{x}), v(\mathbf{x}) \rangle = \int_\Omega u(\mathbf{x}) v(\mathbf{x}) \; d\mathbf{x}.$$

Derivation of the Phase Equations

the operator L_0 has an adjoint

$$(L^* v)(\mathbf{x}) = -v(\mathbf{x}) + f'(u_0(\mathbf{x})) \int_\Omega K(\mathbf{x}-\mathbf{y}) v(\mathbf{y})\, d\mathbf{y},$$

with a nullspace spanned by $v_i^*(\mathbf{x}) = f'(u_0(\mathbf{x}))\partial_i u_0(\mathbf{x}), i = 1, 2$.
For there to exist a solution to

$$(L_0 U_1)(\mathbf{x}, \tau) = \frac{\partial U_0(\mathbf{x}, \tau)}{\partial \tau} - qI(\mathbf{x}) + g \int_0^\tau e^{-(\tau - s)} U_0(\mathbf{x}, s)\, ds,$$

we take v_i^* to be orthogonal to the right hand side.